RESEARCH ARTICLE

ScienceAsia 30 (2004): **365-374**

Simulation of a Circulating Fluidized Bed Combustor with Shrinking Core and Emission Models

Natthapong Ngampradit,[a,*] Pornpote Piumsomboon,[a] and Boonrod Sajjakulnukit[b]

[a] Fuels Research Center, Department of Chemical Technology, Chulalongkorn University, Bangkok, Thailand, 10330.

[b] Department of Alternative Energy Development and Efficiency, Bangkok, Thailand, 10330.

[*] Corresponding author: E-mail: Ng_natthapong@yahoo.com

Received *8 Apr 2004*
Accepted *3 Sep 2004*

ABSTRACT: A Circulating Fluidized Bed Combustor (CFBC) is a highly efficient combustor. It can handle various types of solid fuels such as coal, biomass or agricultural wastes. Coal and biomass have been used as fuel to generate heat for a boiler in many industries. To predict the proper amount of mixed fuel and to reduce the emission from coal burning, a rigorous mathematical model for the CFBC is needed. This paper describes the CFBC model developed as additional subroutines working with ASPEN PLUS version 11.1. The model was divided into three parts: reaction, hydrodynamic, and gas emission. In the first part, the reactions in the combustor were represented by a Continuous Stirred Tank Reactor (CSTR) module. The module was modified by adding the shrinking core model for calculating the size and the weight fraction of particles in each region. In the second part, the hydrodynamics in CFBC were divided into two regions: a lower region with one interval, and an upper region with three intervals. In each region the characteristics, such as the height of the bed, void, and volume, were calculated and sent to CSTR module for adjusting reaction rates in the regions. In the third part, gas emission models were used to calculate the kinetic rates of NO, N_2O and the conversion of SO_2 to predict the emission to the environment.

KEYWORDS: Circulating Fluidized Bed Combustor, Shrinking Core Model, CFBC simulation.

INTRODUCTION

Circulating Fluidized Bed Combustors (CFBCs) are widely used in many industries for steam production and power generation. The advantages of the CFBC are high combustion efficiency, high heat transfer rate, and fuel flexibility. Various kinds of fuel can be used such as coals, biomass and agricultural wastes. The process is also considered to be clean technology, since it has potentials to reduce NO_x and SO_2 emissions. In Thailand, the industries that use such technology are mainly the pulp and paper industries since there are large amounts of agricultural wastes, such as eucalyptus bark, bagasse and pith, left from processes.

Sotudeh-Gharebeagh *et al.*[1] simulated the CFBC for coal combustion using ASPEN PLUS based on an isothermal assumption. The kinetic and hydrodynamic subroutines were used for calculating the rates of reactions and predicting the mean axial voidage profile in upper region. The results expressed in terms of combustion efficiency and emission level. Huilin *et al.*[2] computed a Circulating Fluidized Bed (CFB) boiler with wide particle size distributions by considering the hydrodynamics, heat transfer and combustion of coal. The models predicted the flue gas temperature, the chemical gas species, such as O_2, CO and CO_2, and the char concentration distributions in both axial and radial locations along the furnace. Mukadi *et al.*[3] developed a mathematical model of kinetic reactions to predict gas emissions in an internally CFBC for treatment of industrial solid wastes. Liu and Gibbs[4] presented the model applied to a 12 MW_{th} CFB boiler using a typical wood biomass-pinewood chips as a fuel to predict NO and N_2O emissions. Chen *et al.*[5] developed the model of fluidized bed combustion and studied the emissions of NO_x and N_2O for char combustion, while Winter *et al.*[6] developed the mechanism of NO and N_2O from the single particle of petroleum coke and up to a pilot scale. Natthapong *et al.*[7] presented a model of CFBC with shrinking core model of mixed fuel to predict the size change along a riser.

While most of the previous work focused on either coal or biomass as a fuel, the work in our group has been focused on mixed fuel. In our earlier publication, a CFBC model developed under ASPEN PLUS for various types of fuel, for example, coal, bark, pith or mixed fuel was presented. The model included the shrinking core models for estimating the size change of the solid fuel along the riser. In this paper, the models were extended by including detail reactions of emissions. The emission models, such as the rates of N_2O and NO_x formation and the fractional conversion

of limestone to absorb SO_2, were added. Algorithms for computing the rates and predicting the emissions to the environment were developed.

1. Modeling Approaches

1.1 Assumptions of the Reaction Model

1) The fuel, limestone, and primary air were fed at the bottom of the CFBC with a uniform temperature.

2) The simulated combustor was a rectangular column with the surface area of 36.31 m^2 and the height of 21.84 m (Fig. 1). In the proposed model, the secondary and tertiary air was fed into the combustor at the specified height.

3) The combustion of volatile matters occurred instantaneously at the bottom of the combustor.

4) Char combustion occurred slowly after volatile matters were combusted.

5) Fuel particles and gas temperatures were equal to the bed temperatures varying with respect to the height of the riser.

6) The attrition of the char particles was neglected.

7) All steps of the reactions were calculated with an isothermal at 850 ^{O}C.

1.2 Dimension of CFBC

The model was developed for simulating one of the combustors in a major pulp and paper company in Thailand. The CFBC was divided into two regions: the lower and upper regions. The lower region represented the dense bed, and the upper region the dilute bed fluidization. Each region was composed of kinetic reactions, hydrodynamics and emission sections. In the lower region or the dense bed, the primary air was fed at the bottom of the combustor. The secondary and the tertiary air was fed at the height of 1.703 m and 3.203 m, respectively.

1.3 Simulation Procedures

For the combustion in each region, the combustion of coal particles can be modeled using the following reactions[1]:

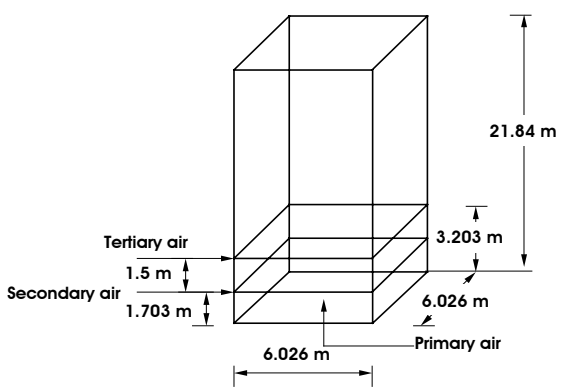

Fig. 1. Dimension of the combustor

1) Devolatilization and volatilite combustion.
2) Char combustion
3) NO_x formation
4) SO_2 absorption

The algorithms of simulations were divided in three parts: reaction, hydrodynamic, and gas emission part. The reaction and gas emission parts were used in the char combustion step. The gas emission part was used to calculate the NO_x formation and SO_2 absorption.

Each reaction will be simulated by using reaction modules of ASPEN, depending on the type of the reactions. All blocks were to be simulated as shown in Fig. 2. The details of the simulations were described as followed.

1.3.1 Devolatilization and Volatilite Combustion.

The yield reactor was used to simulate the decomposition of char or biomass to the constituting components such as carbon, oxygen, hydrogen, nitrogen, sulfur and ash at the lower region.

The stoichiometric reactor (RSTOIC) was used to simulate the volatile combustion processes. Three reactions were considered in this model:

$$C + 0.5O_2 \longrightarrow CO$$
$$S + O_2 \longrightarrow SO_2$$
$$H_2 + 0.5O_2 \longrightarrow H_2O$$

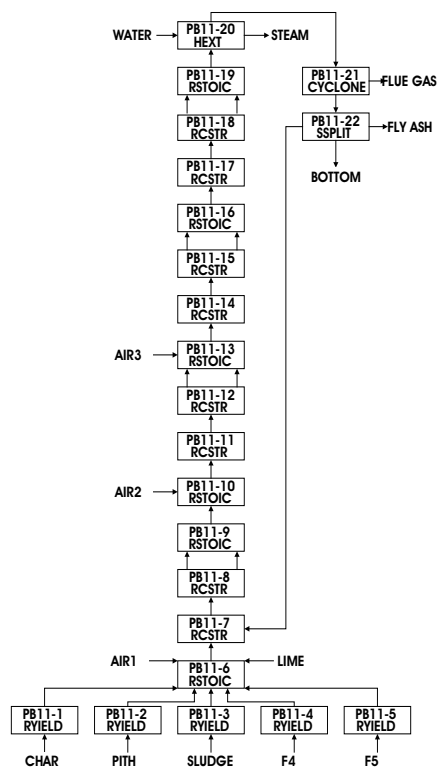

Fig. 2. Simulation diagram for the CFBC

In the first reaction, the volatile carbon fraction reacts with oxygen to form CO only during the volatile combustion process because of the oxygen depletion in the lower region of the riser. For second reaction, 80 percent of sulfur in coal was assumed to be converted to SO_2 during the volatile combustion process. In the last reaction, hydrogen is consumed during the volatile combustion process.

1.3.2 Char combustion.

The Continuous Stirred Tank Reactor (CSTR) was used to model as a well-mixed reaction with known reaction kinetics. Two reactions considered in this reactor are:

$$C + 0.5O_2 \longrightarrow CO$$
$$CO + 0.5O_2 \longrightarrow CO_2$$

The first reaction was a heterogeneous reaction. Then the shrinking core model and the hydrodynamic subroutines were used to calculate rates of reactions, particle size distribution, void and volume of reactor. The flow chart for the calculation was shown in Fig. 3. The second reaction was the homogeneous reaction of CO and O_2.

The emission level of CO from CFBC was strongly dependent on the temperature and reactive concentration. The rate of reaction can be calculated

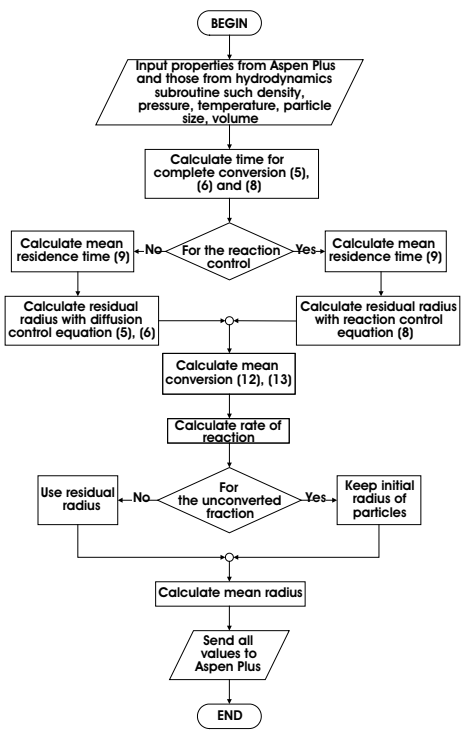

Fig. 3. The basic flowchart for calculating reaction rates and particle sizes for a solid fuel.

using the following equation[1]:

$$Rt_{CO} = 1.18 \times 10^{13} \cdot f_{CO} \cdot f_{O_2}^{0.5} \cdot f_{H_2O}^{0.5} \cdot \left(\frac{P}{R_{g1}T}\right) \cdot \exp\left(-\frac{25000}{R_g T}\right) \cdot C \cdot \varepsilon \qquad (1)$$

where C is the combustion gas concentration ($kmol.m^{-3}$), f is the mole fraction of each component, P is the bed pressure (atm), R_g is the universal gas constant ($kcal.kmol^{-1}.K^{-1}$), R_{g1} is the universal gas constant ($atm.cm^3.g\ mol^{-1}.K^{-1}$), Rt is the rate of reaction ($kmol.m^{-3}.s^{-1}$), T is the bed temperature (K), ε is the void fraction.

1.3.2.1. Shrinking Core Model[9]

The shrinking core model for an isothermal spherical particle is divided into three steps:

1). Diffusion of reactant A from the main body of gas through the gas film to the surface of the solid.

2). Reaction on the surface between reactant A and solid.

3). Diffusion of reaction products from the surface of the solid through the gas film back into the main body of the gas.

In this model the ash layer was absent and did not contribute any resistance. Then the complete conversion time was calculated from above step.

Consider the correlation for estimating the mass transfer coefficient of A, k_{Ag}, for a free-falling spherical particle relative to a fluid, the Ranz and Marshall correlation (1952) relates the Sherwood number, Sh, which incorporates k_{Ag}, to the Schmidt number, Sc, and the Reynolds number, Re,[10]:, according to the following equation:

$$Sh = 2 + 0.6Sc^{1/3}\,Re^{1/2} \qquad (2)$$

That is,

$$\frac{2Rk_{Ag}}{D_A} = 2 + 0.6\left(\frac{\mu}{\rho D_A}\right)^{1/3}\left(\frac{2Ru\rho}{\mu}\right)^{1/2} \qquad (3)$$

where D_A is the diffusion coefficient of A ($m^2.s^{-1}$), k_{Ag} is the mass transfer coefficient of A ($m.s^{-1}$), R is the radius of particle (m), u is the velocity ($m.s^{-1}$), μ is the gas viscosity ($kg.m^{-1}.s^{-1}$), and ρ is the gas density ($kg.m^{-3}$).

This correlation may be used to estimate k_{Ag} given sufficient information about the other quantities.

Rearrange equation (3)

$$k_{Ag} = \frac{D_A}{R} + 0.3D_A \frac{\left(\frac{\mu}{\rho D_A}\right)^{1/3}\left(\frac{2u\rho}{\mu}\right)^{1/2}}{R^{1/2}} \qquad (4)$$

or

$$k_{Ag} = \frac{K_1}{R} + \frac{K_2}{R^{1/2}} \quad (5)$$

With the gas-film mass transfer controls, the complete conversion time can be calculated using the following equations:

Small particles

$$\tau = \frac{\rho_B R^2 f_B}{3bc_{Ag} K_1} \quad (6)$$

where b is the stoichiometric coefficient, c_{Ag} is the concentration of A (kmol.m^{-3}), f_B is the size parameters, and ρ_B is the solid molar density (kmol.m^{-3}).

For large particles

$$\tau = \frac{\rho_B R^{3/2} f_B}{3bc_{Ag} K_2} \quad (7)$$

$$f_B = 1 - \left(\frac{r_c}{R}\right)^3 \quad (8)$$

where r_c is the residual radius (m).

With chemical reaction control, the time for complete conversion is

$$\tau = \frac{\rho_B R}{bk_s c_{Ag}} \quad (9)$$

$$k_s = k_0 \exp\left(-\frac{Ea}{R_{g2} T}\right) \quad (10)$$

where k_0 and E_a were specified by Table 1, E_a is the activation energy (J.kmol^{-1}), k_s is the first order reaction rate constant base on unit surface (m.s^{-1}), k_0 is the frequency factor (m/s), and R_{g2} is the universal gas constant (J.kmol^{-1}.K^{-1}).

The mean conversion for mixed flow of a size mixture of particles of unchanging size, and uniform gas composition is:

$$t = \frac{V(1-\varepsilon)}{F_t} \quad (11)$$

where F_t is the volumetric flow rate of solid (m^3.s^{-1}), t is the residence time (s), and V is the reactor volume (m^3).

Table 1. Kinetic data for each type of fuels.[12,13]

	Frequency factor (m/s)	Activated energy (J/kmol)
Lignite	59600*	1.492 × 10^8
Bagasse	210870*	1.246 × 10^7
Bark	86560*	4.207 × 10^7
Sludge	22140*	4.476 × 10^7

*unit of frequency factor is m/(K×s)

The unconverted fraction of the reactant was given by the following equations[9]:

$$\begin{pmatrix}\text{mean value}\\ \text{for fraction of}\\ \text{B unconverted}\end{pmatrix} = \sum_{\substack{\text{all}\\ \text{sizes}}} \begin{pmatrix}\text{fraction}\\ \text{unconverted}\\ \text{in particles}\\ \text{of size } R_i\end{pmatrix}$$

$$\begin{pmatrix}\text{fraction of}\\ \text{exit or entering}\\ \text{stream consisting}\\ \text{of particles}\\ \text{of size } R_i\end{pmatrix} \quad (12)$$

or in symbols

$$1 - \overline{X}_B = \sum_{R=0}^{R_m} \left[1 - \overline{X}_B(R_i)\right] \frac{F_c(R_i)}{F_c} \quad (13)$$

for gas-film mass transfer control,

$$1 - \overline{X}_B = \sum_{R=0}^{R_m} \left\{ \frac{1}{2!}\frac{\tau(R_i)}{t} - \frac{1}{3!}\left[\frac{\tau(R_i)}{t}\right]^2 + \ldots \right\} \frac{F_c(R_i)}{F_c} \quad (14)$$

where F_c is the mass flow rate of coal (kg .s^{-1}).

For reaction control,

$$1 - \overline{X}_B = \sum_{R=0}^{R_m} \left\{ \frac{1}{4}\frac{\tau(R_i)}{t} - \frac{1}{20}\left[\frac{\tau(R_i)}{t}\right]^2 + \ldots \right\} \frac{F_c(R_i)}{F_c} \quad (15)$$

1.3.2.2. Algorithm of Shrinking-core model

Fig. 3 describes the procedure to calculate the reaction rate, size distribution, and weight fractions of particles for solid fuel of a certain size by using the equations described in the previous section. The first step started with acquiring the physical properties and hydrodynamic data from ASPEN and hydrodynamic subroutine, respectively. The data were used to calculate the rate of the reactions, the time required for complete combustion of the particles in each region of the riser, and the determination of mass transfer or reaction controlled. Then, the mean residence time would be calculated. The time would be used to determine the reaction conversion and the remaining size of the particles after the reaction. Since all of the particles would not be burnt completely, the size of the particles to be passed on the next region would be calculated by averaging the sizes of the unburnt and the burnt fractions. The size of the unburnt fraction would be assumed to be the same as the initial size when the particles moved into the specified region.

1.3.2.3. Hydrodynamic Model

In this paper, the hydrodynamics model described in Sotudeh-Gharebaagh[1] was adopted.

(1) The lower region

In this region, the perfect mixing between the solid

and the gas phase was assumed. The mean void can be considered constant and may be obtained using the correlation of Kunni and Levenspiel(1991)[11].

(2) The upper region

The upper region consists of two zones: an acceleration zone, and a fully developed zone.

The height of the acceleration zone[1] can be find from:

$$Z_{ac} = -\frac{1}{a}\ln\left(\frac{\varepsilon^* - \varepsilon_u}{\varepsilon^* - \varepsilon_{d,avg}}\right) \quad (16)$$

where a is the decay ratio, ε_u is the axial voidage in the acceleration zone, $\varepsilon_{d,avg}$ is the mean voidage of the lower region, and ε^* is the axial voidage at saturated conditions.

The mean axial voidage in the fully developed zone is defined as,

$$\varepsilon_{u,3,avg} = \frac{1}{1 + \frac{\Phi G_s}{U_2 \rho_s}} \quad (17)$$

$$\Phi = 1 + \frac{5.6}{F_r} + 0.47F_{rt}^{0.41} \quad (18)$$

where F_r is the Froude number, F_{rt} is the particle Froude number, G_s is the net solid circulation flux (kg $m^{-2}.s^{-1}$), U_2 is the superficial gas velocity in dilute bed ($m.s^{-1}$), Φ is the slip factor, and ρ_s is the solid density ($kg.m^{-3}$).

In this work, the upper region was divided into three sections for various void fractions as illustrated in Fig. 4.

The mean void fraction in each section of the upper region was calculated from the following equation:

$$\varepsilon_{u,ni,avg} = \varepsilon^* - \frac{1}{a \cdot \Delta L}\left(\varepsilon_{d,avg} - \varepsilon^*\right) \times \left(e^{-a \cdot Z_{ni}} - e^{-a \cdot Z_{ni-1}}\right) \quad (19)$$

1.3.3 NO_x Formation.

CSTR was used to simulate the emission of NO_x and N_2O with respect to the reaction rates following reactions rates[5]:

Formation of NO

$$N_2 + O_2 \longrightarrow 2NO$$

$$Rt_A = K_A C_{O_2} \quad (20)$$

$$K_A = \frac{1000}{3} F_P T \exp(-19000/T) \quad (21)$$

where F_P is the specific surface area (m^{-1}).

Formation of N_2O

$$N_2 + 2NO \longrightarrow 2N_2O$$

$$Rt_B = K_B C_{NO} \quad (22)$$

$$K_B = 3F_P \exp(-9000/T) \quad (23)$$

Reduction of NO by char

$$2NO + 2C \longrightarrow N_2 + 2CO$$

$$Rt_C = K_C C_{NO} \quad (24)$$

$$K_C = 555.6F_P \exp(-14193/T) \quad (25)$$

$$2NO + 2CO \longrightarrow N_2 + 2CO_2$$

$$Rt_D = K_D C_{NO} \quad (26)$$

$$K_D = 5.67x10^3 \exp(-13952/T) \quad (27)$$

Reduction of N_2O by char

$$N_2O + C \longrightarrow N_2 + CO$$

$$Rt_E = K_E C_{N_2O} \quad (28)$$

$$K_E = 13.36F_P \exp(-16677/T) \quad (29)$$

Destruction of N_2O

$$N_2O + CO \longrightarrow N_2 + CO_2$$

$$Rt_F = K_F C_{N_2O} \quad (30)$$

$$K_F = 2.51 \times 10^{11} \exp(-23180/T) C_{CO} \quad (31)$$

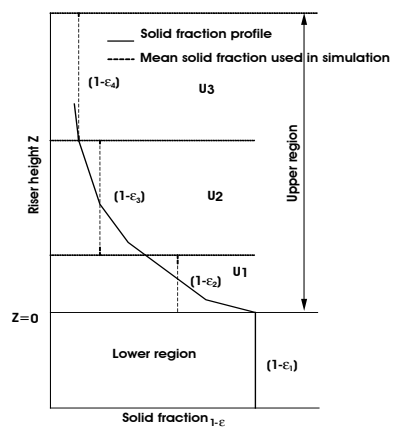

Fig. 4. Variation of void fraction with height in the riser[1]

Thermal decomposition of N_2O

$$2N_2O \longrightarrow 2N_2 + O_2$$

$$Rt_G = K_G C_{N_2O} \quad (32)$$

$$K_G = 1.75x10^8 \exp(-23800/T) \quad (33)$$

The algorithms of NO and N_2O emissions.

Normally, the reactions of NO and N_2O emissions are presented in the network reactions. Most of reaction rates occurred both in series and parallel reactions, while the computer simulations calculated in the sequential reaction. This simulation arranges the rates of reactions in two parts. In the first part, the formation reactions of NO and N_2O were calculated. In the second part, the reduction reactions of NO and N_2O were calculated by considering the rate of reaction, by which the faster reaction was calculated before the slower one.

1.3.4 SO_2 Absorption.

RSTOIC is used to model the capture of sulfur in the CFBC. The SO_2 captured by limestone can be represented by the following reactions:

$$CaCO_3 \longrightarrow CaO + CO_2$$

$$CaO + SO_2 + 0.5O_2 \longrightarrow CaSO_4$$

The fractional conversion of CaO to $CaSO_4$ is strongly affected by the physical and chemical properties of limestone, hydrodynamics parameters, mass transfer resistance, temperature, reactive concentration, particle size distribution and operating condition. The fractional conversion can be calculated from the following expression[1]

$$\frac{V_{CaO}}{1-\varepsilon_I}\left[\frac{t_i - \frac{1}{a_1}\ln\left(1+\frac{3\alpha C Y_{SO_{2,i}}}{R_s K_V}\left(e^{a_1 t_i}-1\right)\right)}{\frac{R_s}{3\alpha C Y_{SO_{2,i}}} - \frac{1}{K_V}}\right] \quad (34)$$

$$\text{where } a_1 = 3.33\times10^{-4}\exp(\gamma R_s) \quad (35)$$

$$\alpha = 35 D_P^{0.3} \quad (36)$$

where D_P is the average sorbent surface particle diameter (cm), K_V is the volumetric rate constant (kmol $m^{-3}.s^{-1}$), R_s is the mean sorbent particle radius (cm), V_{CaO} is the molar volume of CaO ($m^3.kmol^{-1}$), $X_{CaO,i}$ is the fractional conversion of CaO in the ith interval, $Y_{SO_2,i}$ is the mole fraction of SO_2 in the ith interval, α is the external mass transfer coefficient cm. s^{-1}), and ε_i is the porosity of particle after calcinations.

Using equation (34), the moles of SO_2 removed per unit volume become

$$r_{SO_{2,i}} = \frac{V_{CaO}F_1}{1-\varepsilon_I A\Delta L\times100}\left[\frac{t_i - \frac{1}{a_1}\ln\left(1+\frac{3\alpha C Y_{SO_{2,i}}}{R_s K_V}\left(e^{a_1 t_i}-1\right)\right)}{\frac{R_s}{3\alpha C Y_{SO_{2,i}}} - \frac{1}{K_V}}\right] \quad (37)$$

The mean residence time of sorbent particles can be calculated by the following equation.

$$t_1 = \rho_1\sigma_{sp}\frac{AL_1}{F_1} \quad (38)$$

$$\text{and} \quad t_i = \rho_1\sigma_{sp}\frac{A\Delta L}{\xi F_1}\ (i\neq1) \quad (39)$$

where A is the cross section area of combustor (m^2), F_l is the mass flow rate of limestone in the feed (kg s^{-1}), t_i is the mean residence time of sorbent particles in ith interval of the bed (s), and ρ_1 is the density of limestone particles (kg.m^{-3}), σ_{sp} is the volume fraction occupied by sorbent particles, L_1 is the height of dense bed (m), and

$$\xi = \left(1-\sum_2^4 X_{CaO,i-1}\right) \quad (40)$$

Since SO_2 is well mixed in each interval of the bed, an overall SO_2 balance gives

$$Y_{SO_2,1} = \frac{L_1\left(R_{SO_2,1} - r_{SO_2,1}\right)}{CU_1} \quad (41)$$

$$Y_{SO_2,i} = \frac{\Delta L\left(R_{SO_2,i} - r_{SO_2,i}\right)}{CU_2} \quad (42)$$

$$\text{where } R_{SO_2,1} = \frac{F_c W_s}{32AL_1} \quad (43)$$

$$\text{and} \quad R_{SO_2,1} = \frac{\left(1-X_{SO_2,i-1}\right)F_c W_s}{32A\Delta L}\ (i\neq1) \quad (44)$$

where $R_{SO_2,1}$ is the rate SO_2 generation per unit volume of dense bed (kmol.$m^{-3}.s^{-1}$), and W_s is the sulfur weight fraction in dry-based coal.

The fractional sulfur capture for each reactor ($X_{SO_2,i}$) can be calculated from

$$X_{SO_2,1} = 1 - \left[\frac{Y_{SO_2,i} C U_1 A}{F_C \frac{W_s}{32}} \right] \quad (45)$$

$$X_{SO_2,i} = 1 - \left[\frac{Y_{SO_2,i} C U_2 A}{F_C \frac{W_s}{32}\left(1 - X_{SO_2,i-1}\right)} \right] (i \neq 1) \quad (46)$$

Results and Discussion

The fuel included in the simulator were lignite, bagasse, bark and sludge. The proximate and ultimate analyses for each type of fuel are shown in Tables 2 and 3. The simulation results for both single fuel and mixed fuel between lignite and biomass were investigated. In case of mixed fuel, since there are a number of combinations among fuel, the mixtures of bagasse, bark and sludge were selected to demonstrate the model prediction. The kinetic data for calculating the rates of reactions in the RCSTR block are tabulated in Table 1.

The model was used to simulate the operation of a CFBC that produced 110 tons per hour of steam at 510 °C and 110 barg. The fuel to be considered were both single and mixed fuel. In case of single fuel, 4 kg $s^{-1}$of lignite was fed into the combustor. In the other case, the mixed fuel between lignite and biomass were considered. Each simulation of the mixtures decreased the lignite flow rate by 10 %. The flow rate of biomass was increased for keeping the constant of amount of carbon. The results of the simulation are shown in Fig. 5 to 8.

Fig. 5 shows the combustion rates of lignite in mixed fuel for each region in the CFBC, where there were three kinds of mixed fuel and three compositions. All simulation cases showed the same trend. The rates of reactions decreased along the riser height. The reason is that, in the lower region, the carbon concentration was high due to the feed, while in the upper region there was only residual carbon left from the lower region. However in the upper region zone 1, the conversion was closed to zero because of the shortest residence time as shown in Table 4. The conversion in the upper region zone 3 was higher than that in the upper region zone 2, because the residence time in zone 3 was longer than zone 2. Compared with the various ratios of lignite and biomass, the reaction rates of lignite decreased slightly when increased the flow rate of biomass. This is due to the decrease in the concentration of lignite in

Table 2. Proximate analysis for each type of fuel.[8]

Proximate analysis (Wt.%)	Lignite	Bagasse	Bark	Sludge
Moisture	19.86	35.49	39.66	65.42
Fixed carbon	34.85	7.71	9.09	2.9
Volatile matter	34.84	55.23	48.85	13.18
Ash	10.45	1.57	2.4	18.5

Table 3. Ultimate analysis for each type of fuel.[8]

Ultimate analysis (Wt.%)	Lignite	Bagasse	Bark	Sludge
Ash	13.04	2.44	2.82	18.50
Carbon	68.15	48.64	48.40	41.19
Hydrogen	5.09	5.87	6.72	5.40
Nitrogen	1.24	0.16	0.19	1.70
Sulfur	0.59	0.07	0.00	0.72
Oxygen	11.89	42.82	41.87	32.49

Table 4. The results of reactor data for 4.0 kg/s of lignite

Region	Volume (m^3)	Height (m)	Residence time (s)
Lower	61.84	1.70	19009
Upper1	16.70	0.46	1601
Upper2	33.34	0.92	11000
Upper3	681.14	18.76	85544

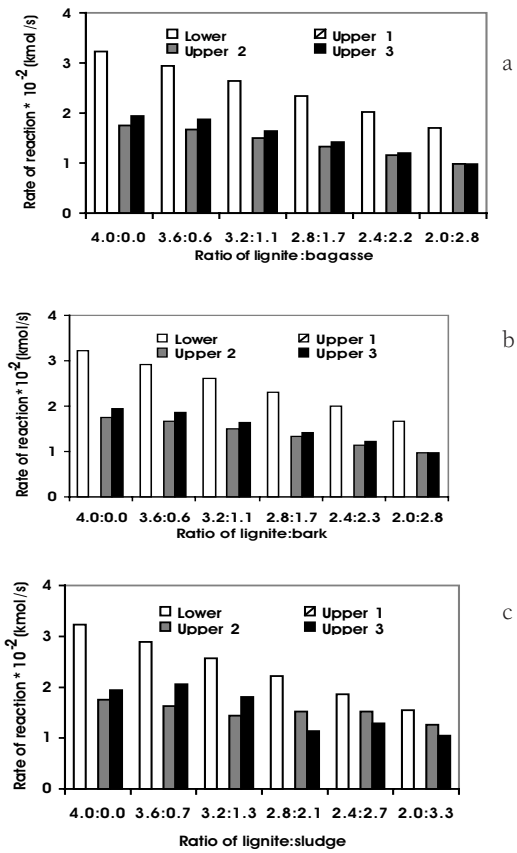

Fig. 5. Rates of the combustion of lignite in mixed fuel for each region in the CFBC: (a) lignite&bagasse, (b) lignite&bark, and (c) lignite&sludge.

the mixed fuel.

Fig. 6 shows the combustion rates of biomass for different types of materials in the mixed fuel. The reaction rates increased with the increase in the fraction in the fuel. For example, at the 2.0:2.8 of lignite and bagasse ratio, the reaction rate increased to 3.87×10^{-2} kmol s^{-1} or about 5 times when compared with the reaction rate at the lignite and bagasse ratio at 3.6:0.6. This is due to the higher concentration of carbon from the biomass. The rates decreased rapidly at high position in the riser since most of the biomass was burnt in the lower region. The reaction rates in the upper region were close to zero. The example for reaction rate of bagasse at 0.6 kmol s^{-1} was shown in Table 5.

Fig. 7 shows the compositions of gas emission when different types of mixed fuel were used. All the simulation cases show the same patterns of responses. For example, Table 6 shows the emissions gas from the lignite and bagasse combustion. The results show that the amount of N_2O was small, which is in agreement with literatures[4,5], while the amount of NO was high when the amount of biomass was increased. This result does not agree with that of Liu *et al.*[14]. This is due to the fact that rate of NO formation in this simulation, equation (20), depended the oxygen concentration only. Then the amount of nitrogen does not affect the NO conversion. However, the amount of CO decreased because of the complete combustion with higher oxygen concentration when the biomass was increased. Finally,

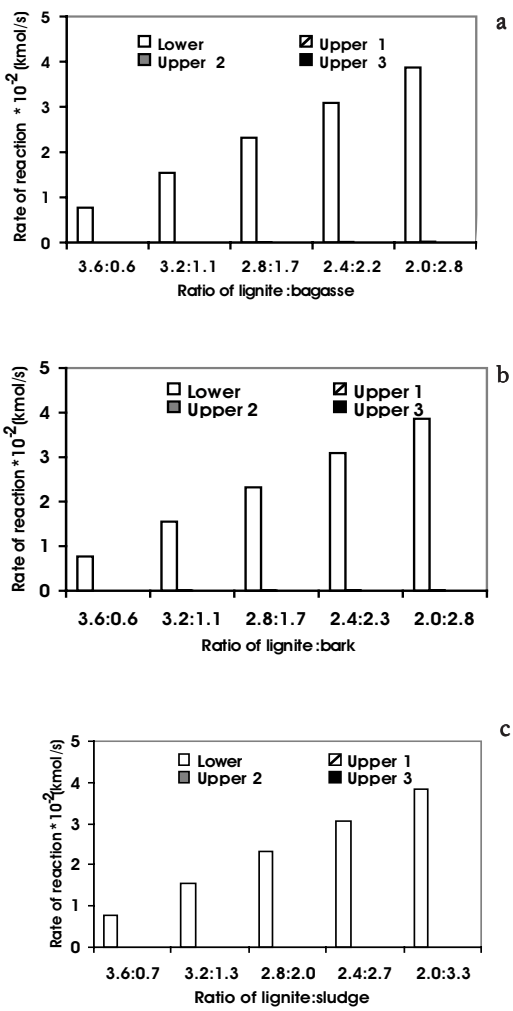

Fig. 6. Rates of the combustion of biomass in mixed fuel for each region in the CFBC: (a) lignite&bagasse, (b) lignite&bark, and (c) lignite&sludge.

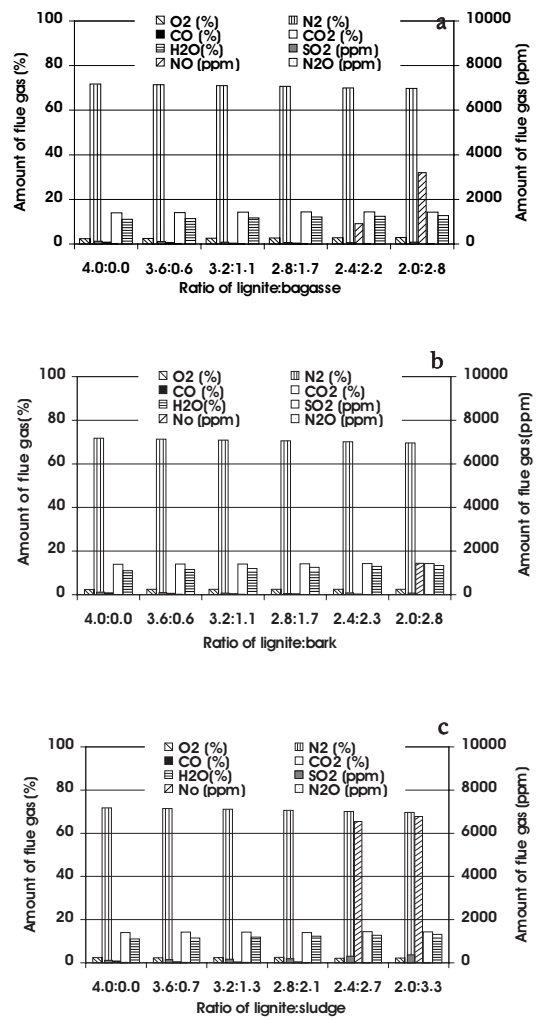

Fig. 7. The composition of flue gas for different kinds of mixed fuel: (a) lignite&bagasse, (b) lignite&bark, and (c) lignite&sludge.

the results also showed that the amount of SO_2 was small

The Prediction of Size Distribution

The example was to demonstrate the size distribution predictions in each region of the riser. The particle sizes of biomass and lignite were divided into 2 and 3 subintervals, respectively. The case shown here was the combustion of single fuel, lignite. The initial radius and weight fraction of lignite are shown in Table 7. The predictions of the size distribution and the weight fraction in each region are shown in Table 8.

In the lower region, where the combustion occurred, most of the smallest particles were burnt. Therefore, its weight fraction almost disappeared. However, the radii of particles did not decrease because the mean residence time was higher than the time to complete conversion. Thus, the algorithm program kept the initial radius for the unconverted particles. For the second interval, weight fraction reduced from 0.52 to 0.16, while that for the third interval increased. This was due to the lower region having small volume, which implied the short residence time. Thus, only the small particles would be burnt completely. The mass of the larger particles reduced more slowly, causing high weight fraction in this interval. Nevertheless, the combustion in this region caused the mean particle size in the third-interval to reduce to 0.0552 m.

The upper region was divided into three regions. The weight fraction of the second-interval particles increased in the first upper regions. The reason is that the large particles had time to reduce their sizes into the second-interval particles.

Since the second and third upper regions had large volume, their residence times would be long. Therefore, most of the small and medium particles were burnt in the regions. Thus, the particles left in these regions were the particles falling in the third-interval size. This observation was noticed with high weight fraction in this interval and the mean particle size was reduced to 0.0524 m as shown in Table 8.

Table 5. Rate of combustion of bagasse at ratio 3.6:0.6

Region	Rate of combustion (kmol/s)
Lower	7.71×10^{-3}
Upper 1	2.65×10^{-5}
Upper 2	1.66×10^{-8}
Upper 3	2.61×10^{-11}

Table 6. The emissions of lignite and bagasse combustion.

Ratio of lignite and bagasse	Amount of gas emission					
	(%)			(ppm)		
	O_2	CO	CO_2	SO_2	NO	N_2O
4.0:0.0	2.42	0.81	13.97	120	1	16
3.6:0.6	2.51	0.59	14.10	101	22	18
3.2:1.1	2.59	0.34	14.26	83	33	18
2.8:1.7	2.69	0.12	14.38	65	41	17
2.4:2.2	2.78	0.01	14.41	51	915	17
2.0:2.8	2.85	0.01	14.31	87	3197	17

Table 7. Initial radius and weight fraction of lignite.

No.	Interval size (m)	Mean initial radius (m)	Weight fraction
1	0-0.001	0.0005	0.08
2	0.001-0.04	0.0205	0.52
3	0.04-0.075	0.0575	0.40

Conclusions

This paper proposed a model for simulating the CFBC using single or mixed fuel. The major improvement from the previous model was the consideration of solid fuel-size change during the combustion. The shrinking core model was included in the simulation to calculate the size distribution and weight fractions in each region of the riser. The modification reflected the phenomena in the riser better than the previous model did. Moreover, the details of emission models were added in the simulation to predict the formation of NO, N_2O, and SO_2. For different biomass fractions in the fuel, the simulation output demonstrated the trend of gas emission, which can be used for environment protection consideration. Although the results from the simulation were not yet validated with the experimental data, the trends of the solution seemed to be reasonable.

Acknowledgements

This research study was supported by the Petroleum

Table 8. The predictions of size distribution and weight fraction in each region.

Region	Volume (m^3)	Mean radius (m)			Weight fraction		
		Interval 1	Interval 2	Interval 3	Interval 1	Interval 2	Interval 3
Lower	61.84	0.0005	0.0205	0.0552	0.0007	0.16	0.84
Upper 1	16.70	0.0005	0.0201	0.0551	0.0116	0.61	0.38
Upper 2	33.34	0.0005	0.0201	0.0524	0.0018	0.15	0.85
Upper 3	681.14	0.0005	0.0201	0.0524	0.0022	0.22	0.78

and Petrochemical Technology Consortium, the Ratchadaphisek Somphot Endowment, and the Graduate School of Chulalongkorn University.

REFERENCES

1. Sotudeh-Gharebaagh R, Legros R, Chaouki J, and Paris J (1998) Simulation of Circulating Fluidized Bed Reactors using ASPEN PLUS. *Fuel* **77**, 327-37.
2. Huilin L, Rushan B, Wenti L, Binxi L and Lidan Y (2000) Computations of a circulating fluidized-bed boiler with wide particle size distributions. *Ind. Eng. Chem. Res* **39**, 3212-20.
3. Mukadi L, Guy C, and Legros R (2000) Prediction of Gas Emissions in an Internally Circulating Fluidized Bed Combustor for Treatment of Industrial Solid Wastes. *Fuel* **79**, 1125-36.
4. Liu H. and Gibbs BM (2002) Modeling of NO and N_2O emissions from biomass-fired circulating fluidized bed combustors. *Fuel* **81**, 271-80.
5. Chen Z, Lin M, Ignowski J, Kelly B, Linjewile TM, and Agarwal PK (2001) Mathematical Modeling of Fluidized Bed Combustion.4: N_2O and NO_x Emission from the Combustion of Char. *Fuel* **80**, 1259-72.
6. Winter F, Loffler G, Wartha C, Hofbauer H, Preto F, and Anthony EJ (1999) The NO and N_2O Formation Mechanism Under Circulating Fluidized Bed Combustor Conditions:from the Single Particle to the Pilot-Scale. *The Canadian Journal of Chemical Engineering* **77,** 275-83.
7. Ngampradit N, Piumsomboon P, and Sajjakulnukit B (2002) Simulation of a Circulating Fluidized Bed Combustor with the Shrinking Core Model Using the Aspen Plus. 9th APCChE Congress and CHEMECA
8. Boiler Plant Design Basis (accessed June 1992) Siam Kraft Industry Co., Ltd., Thailand
9. Levenspiel O (1972) Fluid-particle reactions. In: *Chemical Reaction Engineering, 2nd ed.* pp 357-400 John Wiley & Sons, Singapore.
10. Missen RW, Mims CA, and Saville BA (1999) Multiphase reacting systems. In: *Introduction to Chemical Reaction Engineering and Kinetics*, pp 224-39 John Wiley & Sons, New York, USA.
11. Kunii D and Levenspiel O (1991) High velocity fluidization. In: *Fluidization Engineering*, *2nd ed.* pp193-210 Butterworth-Heinemann, Boston, England.
12. Gaur S and Reed TB (1998) Natural biomass. In. *Thermal Data for Natural and Synthetic Fules* pp102-50 Marcel Dekker Inc, New York, USA.
13. Yamskulna S (2000) "Energy Management System Design for Steam Power Plant," M.Sc. Thesis, Chulalongkorn University, Thailand.
14. Liu DC, Mi T, Shen BX, and Feng B (2002) Reducing N_2O Emission by Co-Combustion of Coal and Biomass (Comm.). *Energy & Fuels* 16, 525-6.